Available online at www.sciencedirect.com
ScienceDirect
Ceramics International 38 (2012) 875–881
CERAMICS INTERNATIONAL
www.elsevier.com/locate/ceramint

Short communication

Facile synthesis of gamma-MnS hierarchical nanostructures with high photoluminescence

Yang Ren, Lian Gao *, Jing Sun, Yangqiao Liu, Xiaofeng Xie

State Key Laboratory of High Performance Ceramics and Superfine Microstructure, Shanghai Institute of Ceramics, Chinese Academy of Sciences, Shanghai 200050, China

Received 30 May 2011; received in revised form 27 June 2011; accepted 8 July 2011
Available online 4th August 2011

Abstract

A facile solvothermal method in the ethylene glycol–H_2O system has been proposed for controllable fabrication of well-crystallized γ-MnS hierarchical nanostructures. In this method, the addition of deionized water into the reaction solution shows a remarkable influence upon the morphology, especially on the preferential orientation growth. Typically, hollow γ-MnS nanospheres could be generated without use of deionized water. However, γ-MnS nanoflowers radially constructed by anisotropic nanorods would be readily obtained with the assistance of deionized water. Moreover, the dosage of deionized water can be used for controlling the crystallinity and particle size of γ-MnS nanoflowers. The role of deionized water played on the growth of γ-MnS nanoflowers has been discussed based on transmission electron microscopy (TEM) and high-resolution TEM (HRTEM). The obtained γ-MnS nanorod-constructed nanoflowers exhibit improved PL property compared to hollow nanospheres, evidenced by the enhanced NBE emission centered at 364 nm.

Keywords: Crystal morphology; MnS; Nanostructures; Solvothermal method

1. Introduction

Manganese sulfide (MnS), a wide gap VIIB-VIA semiconductor, has potential applications in short-wavelength optoelectronic, magnetic semiconductors and luminescent fields [1,2]. MnS occurs in three forms: the stable green α-MnS with rock-salt-type structure and two pink metastable tetrahedral structures, β-MnS (sphalerite type) and γ-MnS (wurtzite type) [3]. Compared with the stable form, metastable phase of MnS is expected to exhibit various properties such as optical, electrical and magnetic properties [4]. Nevertheless, both metastable phases always suffer from thermal instability and tend to transform irreversibly into the stable α-MnS at elevated temperature or pressures [5,6], which drastically causes the loss of property. Consequently, tremendous efforts are being made toward the fabrication of metastable phases (γ-MnS or β-MnS) with excellent quality.

In addition, controlling the architecture of metal sulfide nanocrystals has been of great interests, which is driven primarily by the fact that the properties of semiconductor nanocrystals depend greatly on their shape, size and hierarchy [7–9]. With the intention to fabricate MnS crystallites with desirable architectures, various low-temperature wet chemical solution methods have been developed [10–13], such as a mineral-assisted solvothermal synthesis of metastable γ-MnS crystallites [14], a colloidal route through thermolysis of $Mn(S_2CNEt_2)_2$ molecular precursors in hexadecylamine [15] and a biomolecule-directing synthetic route under hydrothermal conditions [16]. However, most of these approaches were plagued by serious problems, such as complicated process control, unavailable precursors as well as inhomogeneity in morphology/size of the product. Therefore, it is still a great challenge to controllably synthesize MnS crystals with homogenous and well-defined morphologies via facile routes.

In this work, a facile solvothermal method in the ethylene glycol (EG)–H_2O system has been proposed for controllable fabrication of uniform γ-MnS hierarchical nanostructures with good photoluminescence. In this approach, the addition of deionized water into the reaction solution shows a remarkable influence upon the morphology of γ-MnS nanostructures, especially on the preferential orientation growth. γ-MnS nanoflowers radially constructed by anisotropic nanorods are

* Corresponding author. Tel.: +86 21 52412718; fax: +86 21 52413122.
E-mail address: liangao@mail.sic.ac.cn (L. Gao).

0272-8842/$36.00
doi:10.1016/j.ceramint.2011.07.019

obtained in the presence of deionized water, while in the absence of water, hollow γ-MnS nanospheres are prepared. Moreover, the dosage of deionized water can be used for controlling over the crystallinity and particle size of γ-MnS nanoflowers. The obtained γ-MnS nanorod-constructed nanoflowers exhibit greatly improved PL property compared to hollow nanospheres, evidenced by the enhanced NBE emission centered at 364 nm. The present work, achieving fabrication of high-quality γ-MnS hierarchical nanostructures with controlled architectures only by the simple water-tuning solvothermal approach, to the best of our knowledge, has never been reported.

2. Experimental procedures

All chemicals were of analytical grade and used without any treatment (Shanghai Chemical Reagent Co. Ltd., China.). The typical procedure for the synthesis of γ-MnS nanorod-assembled nanoflowers was as follows: 1 mmol $Mn(CH_3COO)_2{\cdot}4H_2O$ (0.245 g), 1.5 mmol sulfur powder (0.048 g) and 1.2 g PVP were added to a vessel that contained 60 mL EG. This was followed with addition of 2 mL distilled water. The above mixture was magnetically stirred for 60 min. The obtained orange solution was then sealed into a Teflon-lined stainless autoclave (100 mL capacity) and kept in an electric oven at 190 °C for 12 h. The autoclave was then taken out and left to cool naturally to room temperature. The resultant pink powder was obtained by centrifugation, washed with water and ethanol three times, and vacuum-dried at 50 °C overnight for characterization. The detailed experimental parameters for the synthesis of typical samples are listed in Table 1.

The products were characterized by transmission electron microscopy (TEM) and high-resolution TEM (HRTEM) (JEM200CX, JEOL, Tokyo, Japan), scanning electron microscopy (SEM, JSM 6700F, Tokyo, Japan) and powder X-ray diffraction (XRD, Rigaku D/max 550 V, Tokyo, Japan, Cu Kα radiation, λ = 0.15406 nm). PL spectra were analyzed by a luminescence spectrometer (LS55, PerkinElmer, CT, USA) at room temperature, with an excitation slit width of 10 nm and an emission slit width of 10 nm.

3. Results and discussion

Fig. 1 shows the XRD pattern of as-prepared samples. Except for sample S6, the diffraction pattern of all the samples are well in accord with wurtzite structured γ-MnS (JCPDS No. 40-1289), indicating that pure γ-MnS can be prepared by such

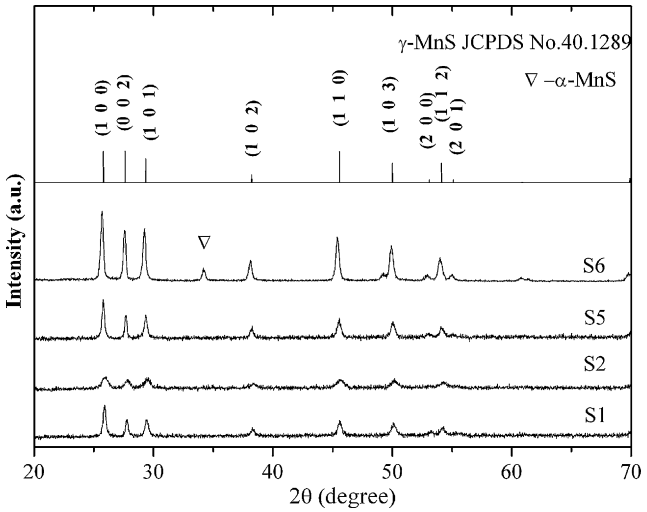

Fig. 1. XRD patterns of the as-prepared samples solvothermally synthesized at 190 °C for 12 h with different amounts of deionized water: S1 (2 ml), S2 (0 ml), S5 (4 ml) and S6 (10 ml), respectively.

simple solvothermal method in EG–H_2O system. The diffraction peak intensity gradually enhances with increasing loading of deionized water, evidencing that the deionized water shows a promotion effect on the crystallization of γ-MnS. Noteworthy, the intensity of some diffraction peaks exhibits remarkable enhancement, especially of (1 0 0) and (1 1 0) planes, indicating that deionized water would possibly facilite the preferential oriented growth of γ-MnS crystallites.

Fig. 2(a) gives the representative SEM image of S1, which demonstrates nearly monodispersed nanoflowers with an average size of about 550 nm. The high-magnification SEM image (inset of Fig. 2(a)) shows that the flower-like nanostructures are composed of radial nanorods. And a hexagonal end face of constructed nanorods can be identified, which is in accord with the crystal habit of the wurtzite structured γ-MnS. Further structural details were studied by TEM and SAED. TEM image (Fig. 2(b)) further shows that the γ-MnS nanoflowers are assembled by nanorods with diameters of ca. 80 nm and lengths of 250–300 nm. The typical SAED pattern (inset of Fig. 2(b)) from single nanorod confirms the well-defined single-crystalline nature. HRTEM image (Fig. 2(c)) shows the lattice fringe along the preferential growth direction of the nanorod. The lattice spacing of 0.316 nm agrees well with the d-spacing of the (0 0 2) planes of γ-MnS, indicating the [0 0 1] preferential growth orientation.

Table 1
Experimental parameters for the synthesis of typical samples (solvothermal temperature was 190 °C for all samples).

Sample	Solvent	*t* (h)	Phase	Morphology	Particles size/nm
S1	EG (60 ml) + H_2O (2 ml)	12	γ-MnS	Flower-like	ca. 550 nm
S2	EG (60 ml)	12	γ-MnS	Hollow spheres	ca. 250 nm
S3	EG (60 ml) + H_2O (2 ml)	4	γ-MnS	Flower-like	ca. 550 nm
S4	EG (60 ml)	4	γ-MnS	Solid and core/shell spheres	ca. 250 nm
S5	EG (60 ml) + H_2O (4 ml)	12	γ-MnS	Flower-like	ca. 600 nm
S6	EG (60 ml) + H_2O (10 ml)	12	γ-MnS + α-MnS	Flower-like + spherical	1–2.5 μm

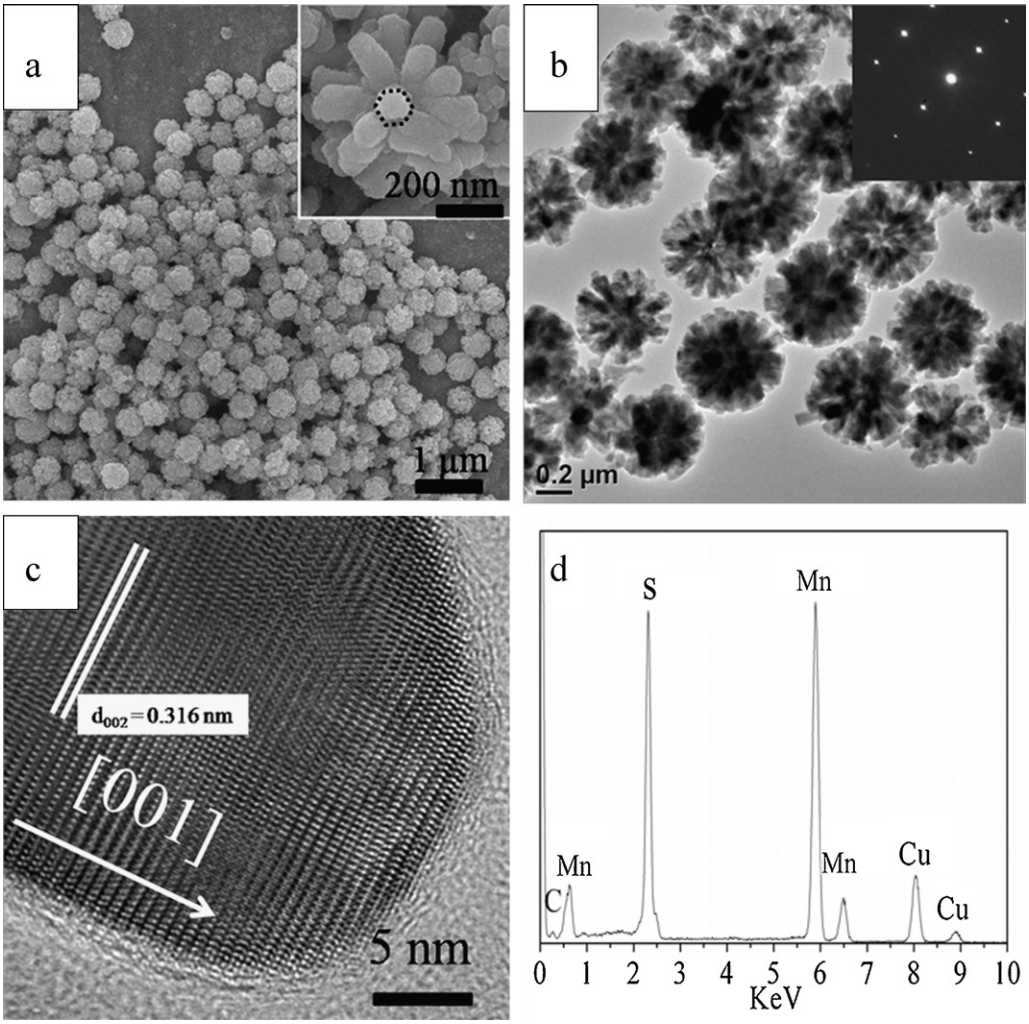

Fig. 2. (a) Low-magnification SEM image of Sample S1 (the inset: high-magnification SEM image of a single nanoflower); (b) TEM image of S1 (the inset: SAED pattern from the primary nanorod); (c) HRTEM image of the nanorod; (d) EDS pattern of the nanoflowers.

The EDS data (Fig. 2(d)) confirm that the product is stoichiometric MnS (atomic ratio Mn:S = 49.52:50.48).

For comparison, we performed the experiment (sample S2) without adding deionized water. Fig. 3(a) and (b) shows the SEM images of S2 under different magnifications. Compact nanospheres with average size of ca. 250 nm are obviously seen. A typical broken nanosphere reveals its hollow nature and that the shell is composed of grain-like nanoparticles with size of ca. 10–15 nm (Fig. 3(c)). The shell thickness of hollow nanospheres is estimated to be ca. 60–100 nm by Fig. 3(d). The SAED pattern (inset of Fig. 3(d)) shows that the shells are polycrystalline. Above results indicate the significant influence of deionized water on the size and morphology of γ-MnS particles in the present reaction system.

As previously reported [2], sulfur powder can be reduced by weak reducing agent ethylene glycol alone via solvothermal process, and then stably generate H_2S to provide S^{2-}. The formation of γ-MnS can be presented as follows:

$$2HOCH_2CH_2OH \xrightarrow{190^\circ C} 2CH_3CHO + H_2O \quad (1)$$

$$2CH_3CHO + S \xrightarrow{190^\circ C} CH_3CO - COCH_3 + H_2S(aq.) \quad (2)$$

$$H_2S + H_2O \rightleftharpoons HS^- + H_3O^+ \quad (3)$$

$$HS^- + H_2O \rightleftharpoons S^{2-} + H_3O^+ \quad (4)$$

$$Mn(Ac)_2 \rightarrow Mn^{2+} + 2Ac^- \quad (5)$$

$$Ac^- + H_2O \rightleftharpoons HAc + OH^- \quad (6)$$

$$Mn^{2+} + S^{2-} \rightarrow MnS\downarrow \quad (7)$$

In order to understand the growth mechanism in the EG–H_2O reaction system, sample S3 was prepared under the same condition as sample S1 except that the reaction time was shortened to 4 h. As shown in Fig. 4(a), imperfect nanoflowers assembled by quasi-rod-shaped nanocrystals are dominant products and their sizes are similar to those of perfect nanoflowers (sample S1). The HRTEM image from the side of the rod-like nanocrystals (Fig. 4(b)) indicates that such rod-shaped structures are composed of adjacent nanoparticles with almost

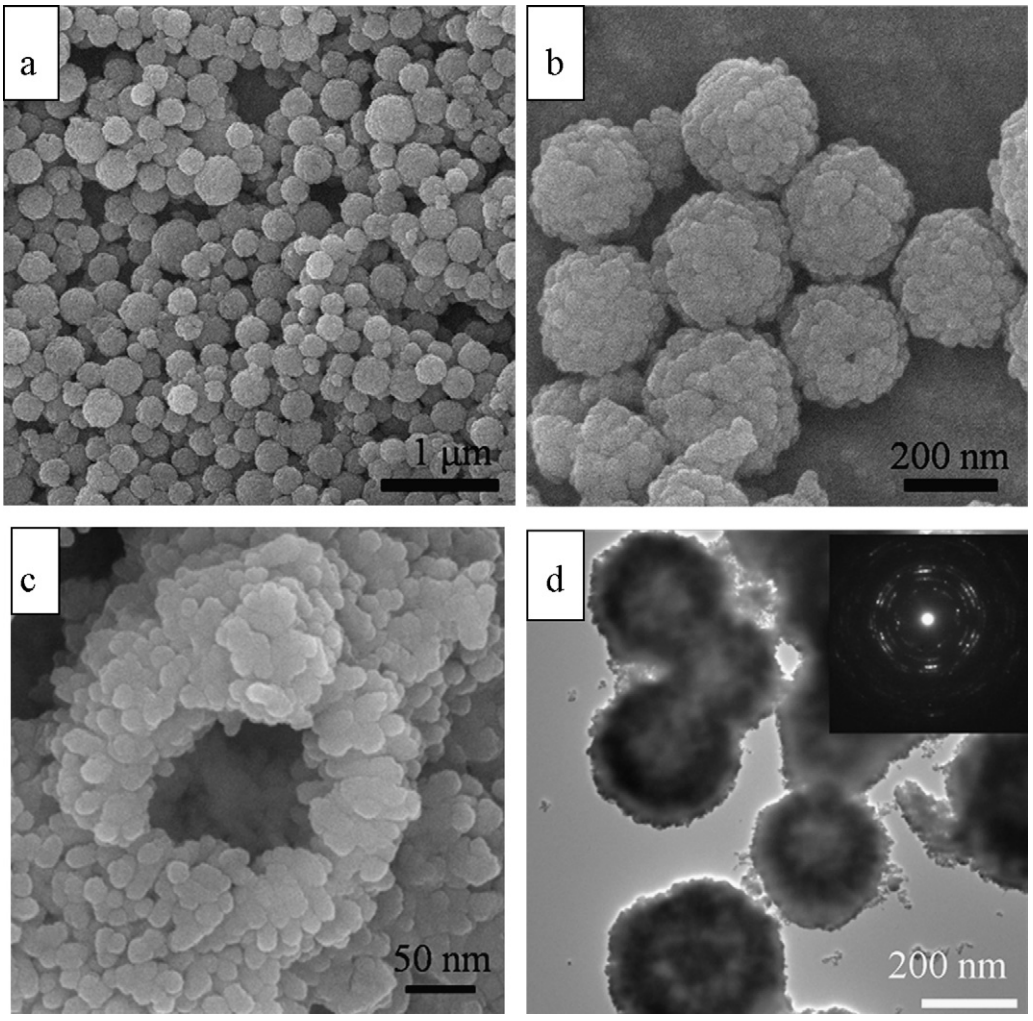

Fig. 3. (a) Low-magnification SEM image of Sample S2; (b) middle-magnification SEM image of S2; (c) high-magnification SEM image of a typical broken nanosphere; (d) TEM image of S2 (the inset: SAED pattern from the ''shell'' region).

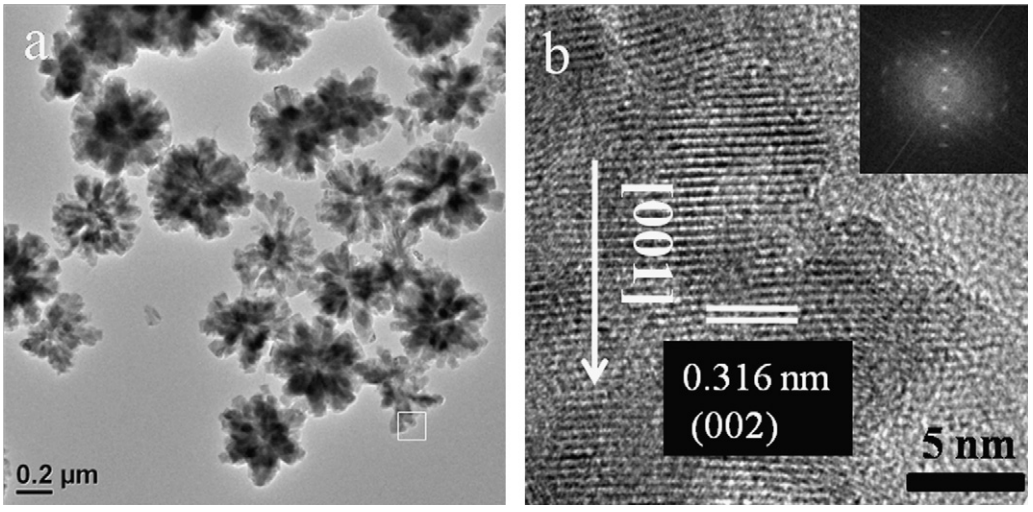

Fig. 4. (a) TEM image of Sample S3; (b) HRTEM image of the primary quasi-rod-shaped nanocrystal (the inset: corresponding FFT image).

the same orientation. The growth orientation evidenced by the interplanar distance is also consistent with that of sample S1. These results suggest that preferential oriented attachment should account for the formation of rod-shaped nanocrystals, especially in the earlier growth stage in the present EG–H_2O system. Although the way that solvent component affects the morphology of products is complicated and multifold, such as the solubility, reactivity, and diffusion behavior, in the present

EG–H_2O system, deionized water, as an additive, plays a role at least from two aspects: First, the deionized water serves as an inducer to promote the ionization of $Mn(Ac)_2$ and H_2S, thus more Mn^{2+} and S^{2-} ions will be generated to form larger quantities of MnS nuclei in the solution. Therefore, the high concentration of growth species (or sufficient supersaturation) further facilitates a fast growth rate, which leads to nanocrystals with higher anisotropy. Second, due to the stronger polarity of H_2O molecules than that of EG molecules, the surface of γ-MnS nanocrystals will be less passivated in the presence of H_2O, therefore, water could also serve as a binder for freshly formed nanocrystallites to orientally grow into a larger crystal (i.e. oriented attachment) [17–19]. Since wurtzite γ-MnS is intrinsically with a polar c-axis, and when the preferential growth is kinetically permitted, growth along this axis is advantaged. As a result, rod-shaped building blocks with [0 0 1] preferential orientation are formed and subsequently self-assembled into flowerlike γ-MnS structures in the presence of surfactant PVP with reduced total system energy [20]. In the later growth stage, Ostwald ripening should also take synergistic effect on the perfect flowerlike structure, which functions as eliminating the oriented attachment-induced defects as well as smoothing the surface of nanocrystals [21]. Finally, well-defined rod-shaped γ-MnS nanocrystals as well as their perfect 3D flowerlike nanostructures are readily fabricated.

Further experiments showed that the size and phase structure of as-obtained particles could be adjusted by increasing the amount of deionized water (Table 1). Generally, the size of as-obtained particles is in direct proportion to the amount of water. When the amount of water increases to 4 ml (sample S5), the size of as-produced γ-MnS flower-like particles increases to ca. 600 nm (Fig. 5(a)–(c)). Concomitantly the diameter of the constructed nanorods increases to ca. 150 nm. When 10 ml of deionized water is introduced into the initial solution (sample S6), flower-shaped particles assembled by well-defined hexagonal-end-faced nanorods as well as some spherical shaped particles are formed, and the size increases to 1–2.5 μm (Fig. 5(d)–(f)). Meanwhile, the product using 10 ml water demonstrates a small portion of α-MnS besides the γ-MnS, as seen from their XRD pattern (S6 in Fig. 1). This result indicates the growth of MnS crystallites might shift to thermodynamic regimes when too much water is added into the reaction solution (10 ml in our case). Thus, the thermodynamically stable α-MnS with spherical shape could be favored through the Ostwald ripening process [15]. Consequently, water plays a key role in controlling the size and phase structure of MnS hierarchical nanocrystals.

When reaction occurs in the absence of deionized water, the nucleation and growth of nanocrystals will be kinetically repressed due to the passivation effect of EG molecule and the high viscosity of EG solvent [22,23]. Thus, grain-like nanocrystals with small sizes are produced (as shown in Fig. 3(c)). In addition, our study indicates that, without the addition of deionized water, the morphology of γ-MnS hierarchical nanostructures evolves from solid nanospheres (4 h, Sample S4) to hollow nanospheres (12 h, Sample S2) during the reaction (Table 1). These results imply that the preferential growth of nanocrystals is kinetically restrained in

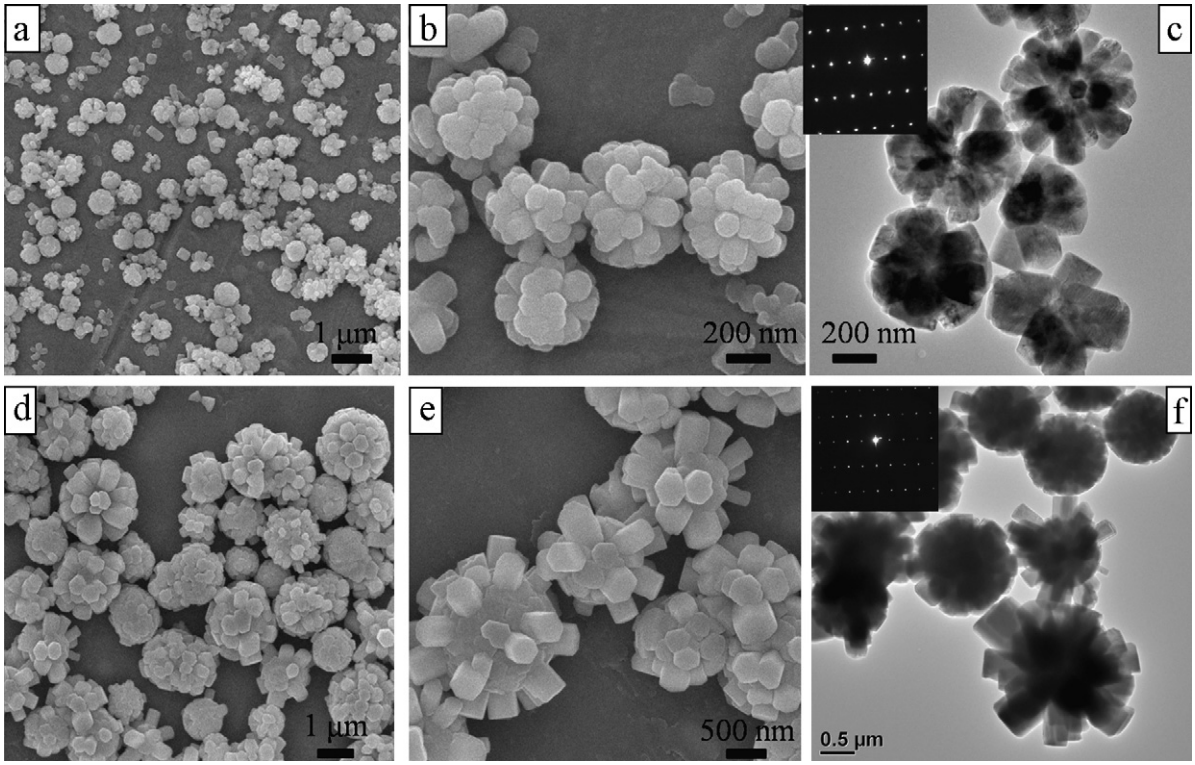

Fig. 5. (a) and (b) SEM images of Sample S5, (c) TEM image of S5 (the inset: SAED pattern of primary nanorod); (d) and (e) SEM images of Sample S6, (f) TEM image of S6 (the inset: SAED pattern from the rod-shaped region).

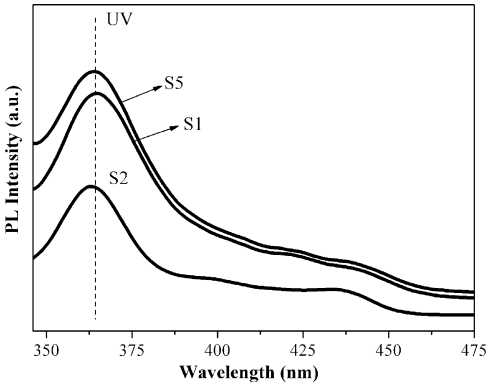

Fig. 6. PL spectra at room temperature (λ_{ex} = 320 nm) of as-obtained γ-MnS hierarchical nanostructures with different sizes: S1, S2 and S5, respectively.

the absence of water, which results in the formation of γ-MnS nanospheres.The PL characterization is an important approach for assessing the quality of semiconductor nanoparticles [15]. Thus, the PL spectra of as-prepared γ-MnS hierarchical nanostructures with different sizes (i.e. S1, S2, S5) were investigated and shown in Fig. 6. It is clear that the PL spectra (λ_{ex} = 320 nm) of all the samples consist of one strong emission centered at 364 nm (3.41 eV) and a weak peak located at around 436 nm (2.85 eV). The former corresponds to the near band-edge (NBE) emission of γ-MnS [15]. The latter one at 436 nm should be attributed to the higher level transition of γ-MnS from the surface states [24]. All the γ-MnS hierarchical nanostructures exhibit dominated NBE emission, indicating their good crystalline quality [15]. Moreover, once deionized water was introduced into the initial solution, the resultant γ-MnS nanoflowers exhibit great enhancement in the NBE emission (S1, S5 in Fig. 6). The highest PL intensity can be obtained for S5 (600 nm γ-MnS nanoflowers) with the addition of 4 ml deionized water. Combined with XRD results (Fig. 1) and TEM observation (Figs. 2(b), 3(d) and 5(c)), it can be concluded that higher crystallinity as well as radiate branched nanostructures would improve the PL property of γ-MnS nanocrystals, since such structured characteristics favor/allow more effective electrons and holes to return to ground state via optically radiative recombination. Similar results can also be found in the literature [25–27]. In addition, a small blue shift of the NBE emissions of S2 (250 nm hollow nanospheres) is observed, which can be ascribed to the size-effect [28]. Thus, the present approach provides as a facile simple method for obtaining γ-MnS nanostructures with excellent luminescent properties.

4. Conclusions

Well-crystallized γ-MnS hierarchical nanostructures with different morphologies (i.e. nanoflowers and hollow nanospheres) and particle sizes have been prepared by a simple solvothermal method in the ethylene glycol–H_2O system. In this method, the addition of deionized water into the reaction solution shows a remarkable influence upon the morphology of γ-MnS nanostructures, especially on the preferential orientation growth. Accordingly, nanorod constructed nanoflowers and hollow nanospheres can be selectively prepared in the presence and absence of deionized water, respectively. As for the formation of γ-MnS nanoflowers, a synergistic growth mechanism combined oriented attachment followed by Ostwald ripening has been proposed by taking into account the kinetic inducing effect of deionized water. Moreover, increasing the dosage of the deionized water would increase the crystallinity and particle size of γ-MnS nanocrystals, and up to a certain amount, phase transformation to α phase occurs. The obtained γ-MnS nanorod-constructed nanoflowers possess improved PL property compared with hollow nanospheres, evidenced by the enhanced NBE emission centered around 364 nm. The synthetic strategy developed in this study may also be extended to fabricate other optical semiconductor nanomaterials with controllable architectures.

Acknowledgments

This work was supported by the National Key Basic Research Development Program of China (973 Program, 2005CB623605) and the National Natural Science Foundation of China (Grant Nos. 50972157 and 51072215).

References

[1] O. Goede, W. Heimbrodt, Optical-properties of (Zn, Mn) and (Cd, Mn) chalcogenide mixed-crystals and superlattices, Phys. Status Solidi B 146 (1) (1988) 11–62.
[2] Y.H. Zheng, Y. Cheng, Y.S. Wang, L.H. Zhou, F. Bao, C. Jia, Metastable gamma-MnS hierarchical architectures: synthesis, characterization, and growth mechanism, J. Phys. Chem. B 110 (16) (2006) 8284–8288.
[3] C. Sombuthawee, S.B. Bonsall, F.A. Hummel, Phase-equilibria in systems ZnS–MnS, ZnS–$CuInS_2$, and MnS–$CuInS_2$, J. Solid State Chem. 25 (4) (1978) 391–399.
[4] Y. Zhang, H. Wang, B. Wang, H.Y. Xu, H. Yan, M. Yoshimura, Hydrothermal synthesis of metastable gamma-manganese sulfide crystallites, Opt. Mater. 23 (1-2) (2003) 433–437.
[5] O. Goede, W. Heimbrodt, V. Weinhold, E. Schnurer, H.G. Eberle, Optical study of phase-transition from tetrahedrally into octahedrally coordinated MnS, Phys. Status Solidi B 143 (2) (1987) 511–518.
[6] B.J. Skromme, Y. Zhang, D.J. Smith, S. Sivananthan, Growth and characterization of pseudomorphic single-crystal zinc blende MnS, Appl. Phys. Lett. 67 (18) (1995) 2690–2692.
[7] R.W.J. Scott, M.J. MacLachlan, G.A. Ozin, Synthesis of metal sulfide materials with controlled architecture, Curr. Opin. Solid State Mater. Sci. 4 (2) (1999) 113–121.
[8] L. Amirav, E. Lifshitz, Spray-produced coral-shaped assemblies of MnS nanocrystal clusters, J. Phys. Chem. B 110 (42) (2006) 20922–20926.
[9] A. Puglisi, S. Mondini, S. Cenedese, A.M. Ferretti, N. Santo, A. Ponti, Monodisperse octahedral alpha-MnS and MnO nanoparticles by the decomposition of manganese oleate in the presence of sulfur, Chem. Mater. 22 (9) (2010) 2804–2813.
[10] S.J. Lei, K.B. Tang, Q. Yang, H.G. Zheng, Solvothermal synthesis of metastable gamma-MnS hollow spheres and control of their phase, Eur. J. Inorg. Chem. (20) (2005) 4124–4128.
[11] F. Zuo, B. Zhang, X.Z. Tang, Y. Xie, Porous metastable gamma-MnS networks: biomolecule-assisted synthesis and optical properties, Nanotechnology 18 (21) (2007).
[12] J. Lu, P.F. Qi, Y.Y. Peng, Z.Y. Meng, Z.P. Yang, W.C. Yu, Y.T. Qian, Metastable MnS crystallites through solvothermal synthesis, Chem. Mater. 13 (6) (2001) 2169–2172.

[13] S.B. Wang, K.W. Li, R. Zhai, H. Wang, Y.D. Hou, H. Yan, Synthesis of metastable gamma-manganese sulfide crystallites by microwave irradiation, Mater. Chem. Phys. 91 (2-3) (2005) 298–300.
[14] X.Y. Zhu, J.F. Ma, J.T. Tao, J. Zhou, Z.Q. Zhao, L.J. Xie, H. Tian, Y.Q. Wang, Mineralizer-assisted solvothermal synthesis of manganese sulfide crystallites, J. Am. Ceram. Soc. 89 (9) (2006) 2926–2928.
[15] Y.W. Jun, Y.Y. Jung, J. Cheon, Architectural control of magnetic semiconductor nanocrystals, J. Am. Chem. Soc. 124 (4) (2002) 615–619.
[16] J.H. Jiang, R.N. Yu, J.Y. Zhu, R. Yi, G.Z. Qiu, Y.H. He, X.H. Liu, Shape-controlled synthesis and properties of manganese sulfide microcrystals via a biomolecule-assisted hydrothermal process, Mater. Chem. Phys. 115 (2-3) (2009) 502–506.
[17] F. Huang, H.Z. Zhang, J.F. Banfield, Two-stage crystal-growth kinetics observed during hydrothermal coarsening of nanocrystalline ZnS, Nano Lett. 3 (3) (2003) 373–378.
[18] F. Huang, H. Zhang, J.F. Banfield, The role of oriented attachment crystal growth in hydrothermal coarsening of nanocrystalline ZnS, J. Phys. Chem. B 107 (38) (2003) 10470–10475.
[19] R.L. Penn, Kinetics of oriented aggregation, J. Phys. Chem. B 108 (34) (2004) 12707–12712.
[20] Y. Li, J. Liu, X. Huang, G. Li, Hydrothermal synthesis of Bi_2WO_6 uniform hierarchical microspheres, Cryst. Growth Des. 7 (7) (2007) 1350–1355.
[21] T. Wang, Z.G. Jin, Y.M. Shi, W.L. Li, J.X. Yang, Kinetic growth of one-dimensional zinc-blende CdTe nanocrystals by aqueous synthesis at low temperature, Cryst. Growth Des. 9 (12) (2009) 5077–5082.
[22] G.Z. Shen, D. Chen, K.B. Tang, X.M. Liu, L.Y. Huang, Y.T. Qian, General synthesis of metal sulfides nanocrystallines via a simple polyol route, J. Solid State Chem. 173 (1) (2003) 232–235.
[23] C. Feldmann, C. Metzmacher, Polyol mediated synthesis of nanoscale MS particles (M = Zn, Cd, Hg), J. Mater. Chem. 11 (10) (2001) 2603–2606.
[24] J. Mu, Z.F. Gu, L. Wang, Z.Q. Zhang, H. Sun, S.Z. Kang, Phase and shape controlling of MnS nanocrystals in the solvothermal process, J. Nanopart. Res. 10 (1) (2008) 197–201.
[25] Y.S. Luo, W.D. Zhang, X.J. Dai, Y. Yang, S.Y. Fu, Facile synthesis and luminescent properties of novel flowerlike $BaMoO_4$ nanostructures by a simple hydrothermal route, J. Phys. Chem. C 113 (12) (2009) 4856–4861.
[26] J. Ota, P. Roy, S.K. Srivastava, B.B. Nayak, A.K. Saxena, Morphology evolution of Sb_2S_3 under hydrothermal conditions: flowerlike structure to nanorods, Cryst. Growth Des. 8 (6) (2008) 2019–2023.
[27] X.J. Dai, Y.S. Luo, S.Y. Fu, W.Q. Chen, Y. Lu, Facile hydrothermal synthesis of 3D hierarchical Bi_2SiO_5 nanoflowers and their luminescent properties, Solid State Sci. 12 (4) (2010) 637–642.
[28] G.C. Wallick, Size effects in the luminescence of ZnS phosphors, Phys. Rev. 84 (2) (1951) 375.